2013

Reflection and transmission from biaxially anisotropic - Isotropic interfaces

Jennifer W. Graham
Syracuse University, jlwarzal@syr.edu

Jay K. Lee
Syracuse University, leejk@syr.edu

Recommended Citation
J. W. Graham and J. K. Lee, "Reflection and transmission from biaxially anisotropic - Isotropic interfaces," Progress in Electromagnetics Research, vol. 136, pp. 681-702, 2013.

Progress In Electromagnetics Research, Vol. 136, 681–702, 2013

REFLECTION AND TRANSMISSION FROM BIAXIALLY ANISOTROPIC — ISOTROPIC INTERFACES

Jennifer W. Graham* **and Jay K. Lee**

Department of Electrical Engineering and Computer Science, Syracuse University, Syracuse, NY 13244, USA

Abstract—In this paper we explore electromagnetic behavior of arbitrarily oriented biaxially anisotropic media; specifically with respect to reflection and transmission. The reflection and transmission of electromagnetic waves incident upon half-space and two-layer interfaces are investigated. The waves may be incident from either the isotropic region or the biaxial region. The biaxial medium considered may be aligned with a principal coordinate system or may be arbitrarily oriented. Critical angle and Brewster angle effects are also analyzed.

1. INTRODUCTION

The study of biaxially anisotropic (or biaxial) materials is of increasing interest. There are several naturally occurring materials with biaxial properties. When we ignore this biaxial nature, we are unable to accurately predict the behavior of circuits using these materials. However, more interesting is the current research in material science. Much of this research has been fueled by electromagnetic interests in a variety of metamaterials. Some studies have shown these materials to have biaxial properties [1, 2]. Despite these interests, theoretical analysis of electromagnetic behavior in biaxial media has not been rigorously studied.

Many authors have studied reflection and transmission in complex materials. Bianisotropic media (in which there is cross-coupling between electric and magnetic fields [3]) has garnered particular attention [4, 5]. In [4] Tsalamengas provides a formulation to compute the reflection and transmission of an arbitrarily polarized wave incident upon a general bianisotropic slab. This slab is described by four tensors, with no limitations on the tensors

Received 8 November 2012, Accepted 7 January 2013, Scheduled 1 February 2013

* Corresponding author: Jennifer W. Graham (jwgraham536@gmail.com).

themselves. Therefore, this formulation could be used to evaluate reflection and transmission coefficients of an arbitrarily oriented biaxial slab. However, we have only one tensor and this formulation is unnecessary. Further, Tsalamengas does not analyze the results or provide numerical examples. In [5] Semchenko and Khakhomov derive and compute reflection and transmission coefficients for unrotated uniaxial bianisotropic material and explore the varying incident wave polarizations. Lee [6] studied wave behavior in tilted and untilted uniaxial media including a detailed study of reflection and transmission from an isotropic-uniaxial interface.

Metamaterials, recently a hot research area, have also been studied for their reflective and refractive characteristics. Grzegorczyk et al. [1, 2] provide an extensive study of the behavior of waves incident upon metamaterial layers. Their work is particularly relevant because they first consider a general bianisotropic medium (with biaxial permittivity and permeability tensors), and then apply the properties of left-handed materials. Therefore, their formulation is general but their results are specific to negative epsilon materials. In fact, the inclusions used to create negative epsilon (or mu) materials make the material anisotropic in general so it is important to understand the anisotropic behaviors. A few researchers have considered reflection and transmission from biaxial boundaries. Stamnes and Sithambaranathan [7] considered reflection and refraction from a plane interface separating an isotropic and a biaxial medium. In their paper, they consider only the unrotated biaxial medium with a diagonal permittivity tensor. Further, they do not present numerical results but rather the formulation of the resulting fields when a plane TE (transverse electric) or TM (transverse magnetic) wave is incident on the interface. Abdulhalim [8] presents a 2×2 matrix approach to solving for reflection and transmission coefficients from biaxial boundaries but does not present any numerical results.

The most extensive work to date on reflection and transmission characteristics in biaxial media is presented by Landry and Maldonado [9, 10]; they study half space reflection and transmission characteristics for biaxial-biaxial, isotropic-biaxial and biaxial-isotropic configurations. They also study 2-layered and multi-layered problems. Their approach is considerably different than the approach presented here. The direction and magnitude of the reflected and refracted waves are treated separately in the half-space case and the 2-layered case is treated by formulating each bounce the incident wave undergoes to compute reflection and transmission coefficients. The multi-layered problem is treated similarly.

In our approach, we expand the plane waves in each medium

then apply the boundary conditions. We use material parameters to determine the directions of each expansion wave and then apply boundary conditions to solve for the magnitude. We apply this treatment to both the half-space and 2-layered problems. This is a familiar and straightforward formulation. Another difference is that we define the electric field vectors in each medium based on the known material parameters (permittivity matrix and rotation matrix) while Landry uses the refractive index and a set of angles to define the relationship between the wave vector and fields. Landry uses a formulation more commonly used in the physics and optics communities and not familiar to most electrical engineers. Our approach is also more general than the approach used in [9, 10]. Finally, we expand upon this research by analyzing the Brewster angle effect and critical angle as functions of permittivity and rotation angles.

We begin by defining the material parameters in Section 1.1. In Section 2, we define the half-space reflection and transmission coefficients of each incident wave on either side of an isotropic-biaxial boundary. We use these results to analyze the critical angle, an analysis that was not considered in [9, 10]. We then go on to formulate the 2-layer case in Section 3 with a wave incident from one isotropic layer onto the biaxial layer. We use these results to analyze the Brewster angle effect which was also not presented in [9, 10]. Conclusions are drawn in Section 4.

1.1. Biaxially Anisotropic Medium Definitions

The defining property of electrically biaxial media is the permittivity tensor. Unlike isotropic materials (with only one permittivity) and uniaxial materials (with 2 different permittivities), biaxially anisotropic materials have three unique values in the permittivity tensor as in

$$\bar{\bar{\varepsilon}} = \begin{bmatrix} \varepsilon_x & 0 & 0 \\ 0 & \varepsilon_y & 0 \\ 0 & 0 & \varepsilon_z \end{bmatrix} \tag{1}$$

Equation (1) represents a biaxial medium whose principal axes are aligned with the laboratory coordinate system. If, however, the biaxial medium is not aligned with some reference coordinate system, the permittivity tensor would not be as simple. We can obtain the tensor for an arbitrarily oriented biaxial medium by applying rotations (Mudaliar and Lee [11]) to the tensor in Equation (1). If the permittivity tensor shown in (1) lies in the double-primed coordinate system, we can transform to the unprimed (laboratory) coordinate system through two rotations: the first about the x'' axis by an angle

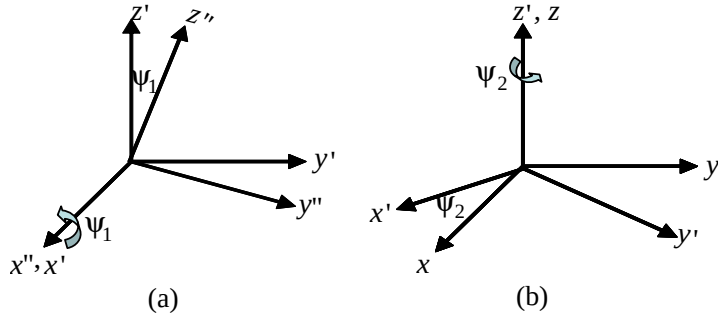

Figure 1. Rotation diagrams.

ψ_1, and the second about the z' axis by an angle ψ_2, as shown in Figures 1(a) and (b), resulting in a full permittivity matrix with all nine elements non-zero in the unprimed system.

The permittivity tensor now is the full matrix where

$$\begin{aligned}
\varepsilon_{xx} &= \varepsilon_x \cos^2\psi_2 + \left(\varepsilon_y \cos^2\psi_1 + \varepsilon_z \sin^2\psi_1\right)\sin^2\psi_2 \\
\varepsilon_{xy} &= \left(-\varepsilon_x + \varepsilon_y \cos^2\psi_1 + \varepsilon_z \sin^2\psi_1\right)\sin\psi_2\cos\psi_2 \\
\varepsilon_{xz} &= \left(\varepsilon_z - \varepsilon_y\right)\sin\psi_1\cos\psi_1\sin\psi_2 \\
\varepsilon_{yy} &= \varepsilon_x \sin^2\psi_2 + \left(\varepsilon_y \cos^2\psi_1 + \varepsilon_z \sin^2\psi_1\right)\cos^2\psi_2 \\
\varepsilon_{yz} &= \left(\varepsilon_z - \varepsilon_y\right)\sin\psi_1\cos\psi_1\cos\psi_2 \\
\varepsilon_{zz} &= \varepsilon_y \sin^2\psi_1 + \varepsilon_z \cos^2\psi_1 \\
\varepsilon_{yx} &= \varepsilon_{xy},\ \varepsilon_{zx} = \varepsilon_{xz},\ \varepsilon_{zy} = \varepsilon_{yz}
\end{aligned} \tag{2}$$

Another important electromagnetic property of biaxially anisotropic media is birefringence. If a wave is incident upon a biaxial medium, two characteristic waves will be refracted, the so called *a-wave* and *b-wave* [11].

2. HALF SPACE REFLECTION AND TRANSMISSION COEFFICIENTS

In general, the study of half-space (one interface) reflection and transmission problems can be broken down into four main configurations as noted by Pettis [12, Appendix G]. These configurations are listed in Table 1.

To derive the half-space reflection and transmission coefficients, we formulate the fields in each region of interest, apply the boundary conditions and solve for the reflection and transmission coefficients.

Table 1. Half-space configurations.

Case	Configuration
1	horizontal or vertical wave downward incident on isotropic-biaxial interface
2	a-wave or b-wave upward incident on biaxial-isotropic interface
3	a-wave or b-wave downward incident on biaxial-isotropic interface
4	horizontal or vertical wave upward incident on isotropic-biaxial interface

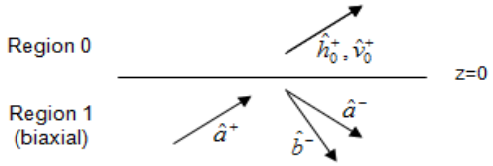

Figure 2. A-wave incident upon biaxial-isotropic interface.

2.1. Derivation of Half-space Coefficients

In this section we derive the half space coefficients for Case 2 (see Table 1), as an example. Note that the derivation of the coefficients for Case 1 was presented in [13] and this derivation follows the same steps. Consider an upward propagating a-wave incident from region 1 upon region 0. This incident wave will generate two downward propagating reflected waves (an a-wave and a b-wave in the biaxial medium) and two upward propagating transmitted waves (one horizontally polarized and one vertically polarized in the isotropic region). This phenomenon is depicted in Figure 2. Region 0 has isotropic permittivity ε_o and region 1 has the permittivity tensor given by (2). Both regions have permeability μ_o.

The first step is to formulate the fields in each region to solve for the half-space coefficients. Assuming time harmonic ($e^{-i\omega t}$) plane wave incidence with unit amplitude we can write

$$\begin{aligned} \bar{E}_1(\bar{r}) &= \hat{a}^+ e^{i\bar{k}_a\cdot\bar{r}} + \hat{a}^- R_{aa}^{10} e^{i\bar{\kappa}_a\cdot\bar{r}} + \hat{b}^- R_{ab}^{10} e^{i\bar{\kappa}_b\cdot\bar{r}} \\ \bar{E}_0(\bar{r}) &= \hat{h}_0^+ X_{ah}^{10} e^{i\bar{k}_0\cdot\bar{r}} + \hat{v}_0^+ X_{av}^{10} e^{i\bar{k}_0\cdot\bar{r}} \end{aligned} \tag{3}$$

where k-vectors are used for upward propagating waves (propagating in

the $+z$ direction) and κ-vectors are for downward propagating waves. Note that there are four distinct values for k_z in this region: two for each a-wave and two for each b-wave. A single fourth order equation, known as the *Booker quartic*, provides the solutions for these propagation constants. We will use the *Booker quartic* equation derived by Pettis [12] for k_z, given by

$$\varepsilon_{zz}k_z^4 + \Delta k_z^3 + \Sigma k_z^2 + Xk_z + \Gamma = 0 \tag{4}$$

where the coefficients ε_{zz}, Δ, Σ, X, and Γ are defined by Pettis [12, Appendix I]. We are defining the reflection coefficients, R_{ij}^{mn}, such that m is the incident region, n is the transmission region, i is the incident wave polarization and j is the reflected wave polarization. The transmission coefficients, X_{ij}^{mn}, are defined the same way with j as the transmitted wave polarization. The electric field unit vectors are defined such that $\hat{h}$ is the horizontally polarized (or TE) wave unit vector, $\hat{v}$ is the vertically polarized (or TM) wave unit vector, $\hat{a}$ is the a-wave electric field unit vector and $\hat{b}$ is the b-wave electric field unit vector. We define $\hat{h}$ and $\hat{v}$ in the same manner as Kong [3] and use the equations he presented to calculate the unit vectors. The a-wave is defined as the characteristic wave in the biaxial medium that has the smaller wave number; the b-wave has the larger wave number. The superscript on the unit vectors indicate whether the wave is upward propagating (positive sign) or downward propagating (negative sign). Finally, the subscript on the isotropic unit vectors indicates which region the unit vector is in to differentiate when we consider the 2-layered problem.

The four unknown coefficients at the half-space boundary are evaluated by applying the boundary conditions on the electric fields and magnetic fields given by.

$$\hat{z}\times\bar{E}_0(\bar{r}) = \hat{z}\times\bar{E}_1(\bar{r}), \quad \text{at } z=0 \tag{5}$$

$$\hat{z}\times\bar{H}_0(\bar{r}) = \hat{z}\times\bar{H}_1(\bar{r}) \longrightarrow \hat{z}\times\nabla\times\bar{E}_0(\bar{r}) = \hat{z}\times\nabla\times\bar{E}_1(\bar{r}), \quad \text{at } z=0 \tag{6}$$

Applying the electric field boundary condition, the cross product of the normal with the electric fields in regions 1 and 0 are computed. The resulting tangential electric fields are set equal to each other. Like components are combined and resulting terms are rearranged to obtain two equations. This process is repeated with magnetic field boundary condition. Evaluating the curl using the propagation vector cross product, the tangential magnetic field is computed in both regions and set equal to each other (assuming no source at the boundary). Two additional equations are obtained yielding a set of four equations for the four unknown coefficients. We can then write the four equations

in matrix form

$$\begin{bmatrix} -a_y^- & -b_y^- & h_{oy}^+ & v_{oy}^+ \\ -a_x^- & -b_x^- & h_{ox}^+ & v_{ox}^+ \\ -\left(k_x a_z^- - k_z^{ad} a_x^-\right) & -\left(k_x b_z^- - k_z^{bv} b_x^-\right) & \left(k_x h_{oz}^+ - k_{0z} h_{0x}^+\right) & \left(k_x v_{oz}^+ - k_{0z} v_{0x}^+\right) \\ -\left(k_y a_z^- - k_z^{ad} a_y^-\right) & -\left(k_y b_z^- - k_z^{bv} b_y^-\right) & \left(k_y h_{oz}^+ - k_{0z} h_{0y}^+\right) & \left(k_y v_{oz}^+ - k_{0z} v_{0y}^+\right) \end{bmatrix}$$

$$\begin{bmatrix} R_{aa}^{10} \\ R_{ab}^{10} \\ X_{ah}^{10} \\ X_{av}^{10} \end{bmatrix} = \begin{bmatrix} a_y^+ \\ a_x^+ \\ \left(k_x a_z^+ - k_z^{au} a_x^+\right) \\ \left(k_y a_z^+ - k_z^{au} a_y^+\right) \end{bmatrix} \tag{7}$$

This matrix can be solved numerically to obtain the half-space reflection and transmission coefficients for this configuration. This derivation procedure is applied to each case given in Table 1 and results are provided. A more detailed procedure is shown in [13] for case 1.

2.2. Evaluation of Reflection and Transmission of Wave Incident from Region 0

The first case studied is Case 1; an electromagnetic wave is incident from the isotropic medium (region 0) to the anisotropic medium (region 1). First, we define the angle of incidence for the half space problem such that $\hat{z}$ is normal to the boundary. The incident wave propagation vector can have any orientation. The geometry of this half space case in the plane of incidence (defined by φ) with angle of incidence θ, is shown in Figure 3.

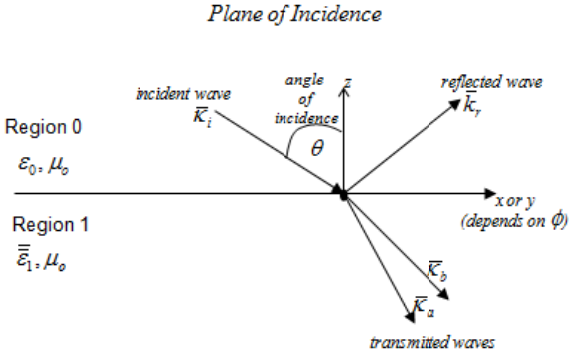

Figure 3. Diagram of plane and angle of incidence for wave incident from region 0.

Due to the phase matching condition, k_x and k_y are continuous across the boundary. We will use k_x and k_y to compute two k_z values (one for each characteristic wave) in region 1 using the Booker quartic from Equation (4).

In this first half-space problem case, we consider the plane of incidence to be the y-z plane ($\varphi = 90°$). The isotropic medium is again air and the biaxial medium is unrotated with relative permittivity tensor with permittivities $\varepsilon_x = 2$, $\varepsilon_y = 5$, and $\varepsilon_z = 8$. The reflection and transmission coefficients are plotted against angle of incidence in Figure 4(a). Considering first the co-polarized reflection coefficients, we observe that at smaller angles, the vertically polarized wave is reflected more strongly than the horizontally polarized wave. For angles greater than approximately 40°, this behavior is reversed and the horizontally polarized wave is reflected more strongly. This is in contrast with the typical behavior at an isotropic-isotropic half space boundary where the horizontally polarized wave is reflected more strongly for all incident angles. We can also observe the Brewster angle effect. At an incident angle just above 60°, the vertically polarized wave has zero reflection and only the horizontally polarized wave is reflected. The Brewster angle effect will be discussed in more detail. For this case, the cross-polarized reflection coefficients (R_{hv}, R_{vh}) are nearly zero. This is consistent with the behavior at an isotropic-isotropic interface. Analyzing the transmission coefficients we observe that when the horizontally polarized wave is incident, the energy is transmitted to the a-wave but not the b-wave as X_{hb} is approximately zero. Similarly, the vertically polarized wave transmits energy into the b-wave with X_{va} approximately zero. The X_{ha} and X_{vb} behave like co-polarized transmission coefficients while X_{hb} and X_{va} behave like cross-polarized transmission coefficients. In this manner, the a-wave is acting like a horizontally polarized wave and the b-wave is acting like a vertically polarized wave for the given medium parameters and plane of incidence.

Consider the same problem when region 2 is rotated such that ψ_1 and ψ_2 are 45°. Given this new biaxial medium, first consider the co-polarized reflection coefficients shown in Figure 4(b). The relative behavior has changed. For all incident angles, the horizontally polarized wave is reflected more strongly than the vertically polarized wave. Also of interest are the cross-polarized reflection coefficients which, while small, are no longer zero. This means that a horizontally polarized wave will reflect both horizontally and vertically polarized waves. This behavior is not observed at an isotropic-isotropic boundary. The transmission coefficients are also affected by this rotation. Energy is transmitted to both the a-wave and b-wave when

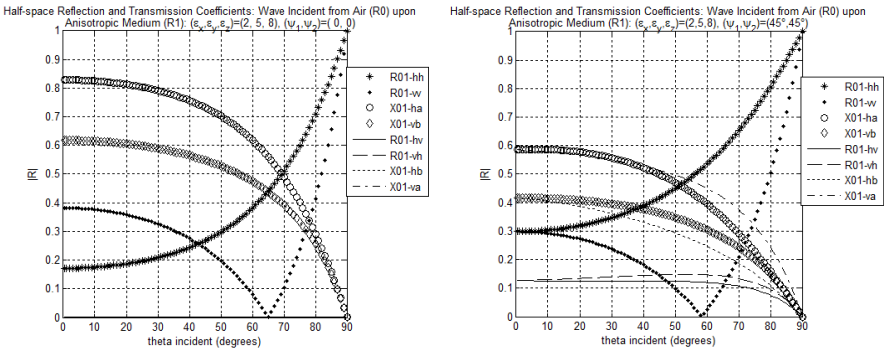

Figure 4. Half-space coefficients for incident wave from isotropic medium to biaxial medium (ε_x, ε_y, ε_z) = (2, 5, 8); (a) unrotated, (b) rotated, (ψ_1, ψ_2) = (45°, 45°).

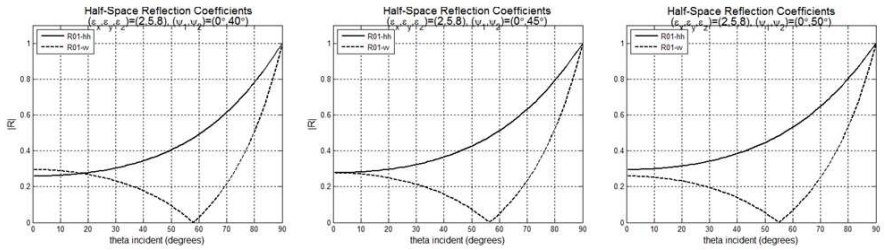

Figure 5. Half-space co-polarized reflection coefficients for incident wave from isotropic medium to biaxial medium (ε_x, ε_y, ε_z) = (2, 5, 8), (ψ_1=0, ψ_2 varied).

either the horizontally polarized wave or vertically polarized wave is incident. We can conclude then a wave incident upon a rotated biaxial medium from an isotropic medium it will generate two transmitted (*double refraction*) and two reflected waves.

In the unrotated case, we observed the unique behavior of the horizontally polarized wave being reflected less than the vertically polarized wave. Upon rotation this behavior is no longer present. This behavior is further investigated. As ψ_1 increases from 0°, R_{hh} is not significantly changed while R_{vv} increases thus enhancing the unique behavior. However, when we increase ψ_2 we see more significant results. As ψ_2 increases from 0° R_{hh} increases and R_{vv} decreases. When ψ_2 reaches 45° R_{hh} and R_{vv} are equal at an incidence angle of 0° and diverge as the angle of incidence increases. When ψ_2 increases beyond 45°, the difference between R_{hh} and R_{vv} at low angle increases with R_{hh} always greater than R_{vv}. This behavior is shown in Figure 5.

2.3. Critical Angle Analysis

The critical angle is related to the phenomenon of total internal reflection. When the angle of incidence is larger than the critical angle, we have total reflection [3]. Total internal reflection is an important practical phenomenon as it is used to implement dielectric waveguides such as fiber optic cables. This phenomenon occurs when the transmitted wave becomes evanescent. Evanescence occurs when the propagation vector becomes imaginary, so as the wave travels into the transmission medium, it decays as $e^{\alpha z}$, where α is the imaginary part of the propagation vector for the wave traveling in the $-z$ direction. Therefore, the critical angle is the angle of incidence for which the propagation vector becomes imaginary. We have chosen a boundary between two real materials to demonstrate the critical angle effect. The incident wave is propagating in Silicon which has a relative permittivity of approximately 12. The transmission medium is PTFE cloth (Teflon), which is biaxially anisotropic with relative permittivities $\varepsilon_x = 2.45$, $\varepsilon_y = 2.89$, and $\varepsilon_z = 2.95$. The co-polarized half-space reflection coefficients from the silicon-PTFE cloth are shown in Figure 6. In this figure, the reflection coefficients go to 1 at approximately 30°. This is the phenomenon of total internal reflection.

We also considered the behavior of the critical angle as the permittivity tensor is rotated. In the first case, permittivity rotations are about the z-axis (ψ_2) with no rotation about the x-axis ($\psi_1 = 0$) in a plane of incidence described by φ_i of 0° (x-z plane), 25° and 90° (y-z

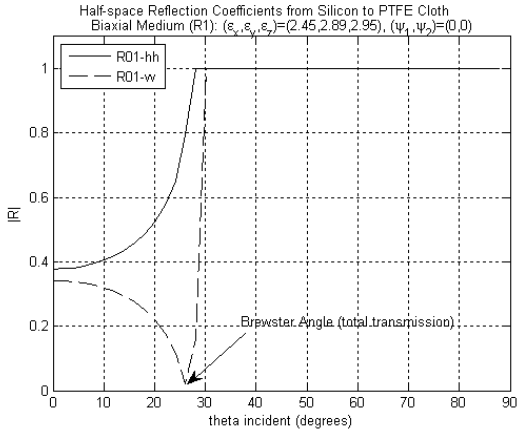

Figure 6. Co-polarized reflection coefficients from Silicon-PTFE cloth boundary.

plane). The results showed that when the medium is rotated about the z-axis, the critical angle varies by less than 5°. When the plane of incidence is changed, the critical angle behavior changes but the peak-to-peak variation over ψ_2 does not change. In the second case, we consider rotations about the x-axis (ψ_1) with no rotation about the z-axis ($\psi_2 = 0$) and the same incidence planes. The results for this case revealed that when the medium is rotated about the x-axis, the critical angle varies by less than 1° when φ_i is 25° and not at all for other incident planes.

2.4. Brewster Angle Effect

The Brewster angle is defined as the angle of incidence for which there is no reflected power. At an isotropic-isotropic half-space boundary, the vertically polarized (transverse magnetic, TM) wave generally experiences zero reflection at some angle. The horizontally polarized (transverse electric) wave generally reflects more than the vertical wave and has non-zero reflection for all angles. The result is that when an unpolarized wave (with both vertical and horizontal polarizations present) is incident upon a boundary at the Brewster angle the reflected electromagnetic wave will be linearly polarized (with horizontal polarization).

The Brewster angle has not been extensively studied for arbitrarily oriented biaxial media. We can see the Brewster angle effect in Figures 4(a) and (b). Figure 4(a) shows that for an incident angle of approximately 62°, only the horizontally polarized wave is reflected; the vertically polarized wave is not reflected at all (reflection coefficient goes to zero). When we rotated the medium as shown in Figure 4(b), the Brewster angle is approximately 57°. Thus we conclude that the Brewster angle depends on rotation of the permittivity tensor.

2.5. Evaluation of Reflection and Transmission of Wave Upward Incident from Region 1

Now we want to repeat the analysis in Section 2.2 for a wave incident from region 1. The plane of incidence and angle of incidence are shown in Figure 7.

We analyzed the same interface considered by Landry and Maldonado [9]. They consider the biaxial-isotropic half-space as a special case. The biaxial relative permittivity tensor under consideration has permittivity values of $(\varepsilon_x, \varepsilon_y, \varepsilon_z) = (1.2^2, 1.7^2, 2.2^2)$. Landry and Maldonado defined three counter clockwise rotations, first around the z-axis (ψ_0), then around the x-axis (ψ_1) and finally again around the z-axis (ψ_2). We modified our equations to accommodate

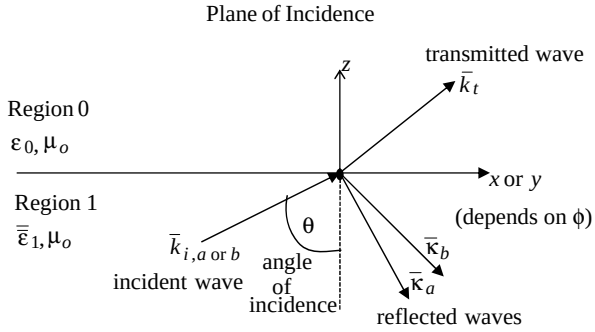

Figure 7. Diagram of plane and angle of incidence for wave incident from region 1.

this additional z-axis rotation (ψ_0) and set $\psi_0 = \psi_1 = 75^\circ$ and $\psi_2 = -75^\circ$. The wave is incident in the x-z plane ($\varphi_i = 0^\circ$) while the angle of incidence ranges from -25° to 25° (where the negative angles are equivalent to $\varphi_i = 180^\circ$. Using this permittivity tensor, we calculate reflection and transmission coefficients for an upward propagating a-wave and b-wave. In Landry and Maldonado's terminology, the a-wave is defined by the inner sheet wave vector surface and the b-wave is defined by the outer sheet wave vector surface.

The half-space reflection and transmission coefficients for both cases (upward incident a-wave and b-wave) exactly match those published by Landry and Maldonado [9, Figure 11]. Observations from their paper and our results include first that an incident a-wave will reflect both an a-wave and a b-wave back into the biaxial medium unless it is normal incidence. Also, the reflection and transmission coefficients are not symmetric about the normal incidence point due to the rotation of the permittivity matrix. This means that the reflection behavior is different in the x-z plane ($\varphi_i = 0^\circ$) and the $-x$-z plane ($\varphi_i = 180^\circ$). Finally, both the reflected and transmitted field strength is stronger for the b-wave as compared to the a-wave.

Having verified our results with the published results of Landry and Maldonado [9], we consider the same half-space configuration where the biaxial medium has permittivities of $\varepsilon_x = 2$, $\varepsilon_y = 5$, and $\varepsilon_z = 8$. Here, the plane of incidence has changed such that $\varphi = 0^\circ$. As we did in the previous analysis, we start with an unrotated biaxial medium. To make sense of the incident wave definitions, we consider only the a-wave incidence here, though we have analyzed b-wave incidence that shows similar behavior to a-wave incident case. The reflection coefficients are plotted against angle of incidence in

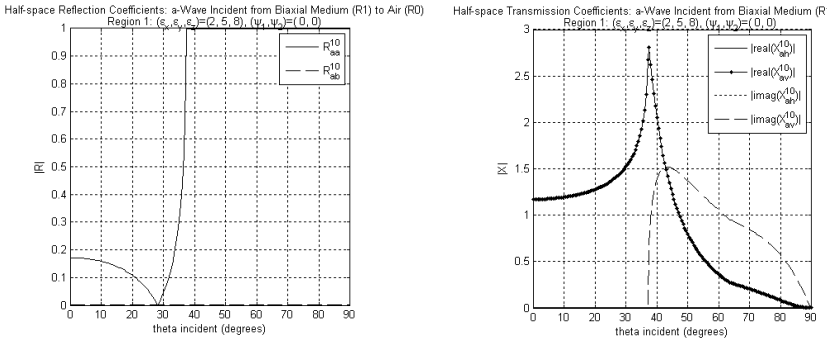

(a) (b)

Figure 8. Reflection and transmission coefficients for a-wave upward incident upon biaxial-air half-space. Biaxial parameters: (ε_x, ε_y, ε_z) = (2, 5, 8), (ψ_1, ψ_2) = (0°, 0°).

Figure 8(a). Observe total internal reflection with R_{aa} equal to 1 above the critical angle of 37.5°. The Brewster angle effect is also evident where R_{aa} goes to zero at an incident angle of 28°. Finally, the cross-polarized reflection coefficients R_{ab} is approximately zero, a behavior observed at an isotropic-isotropic boundary.

Also observe half-space transmission coefficients shown in Figure 8(b) (φ = 0°). When the a-wave is incident the energy is transmitted to the vertically polarized wave and X_{av} behaves like co-polarized transmission coefficient. There is no energy transmitted to the horizontally polarized wave as X_{ah} behaves like a cross-polarized transmission coefficient with values close to zero. This polarization pairing is opposite of what we observed when the incident wave was from region 0 (see Figure 4). If the plane of incidence is changed, such that $\varphi = 90°$, the a-wave is transmitted to the h-wave, as it was for the same plane of incidence when the wave was incident from region 0. The reason for this behavior is that the horizontally polarized and vertically polarized waves are defined with reference to the plane of incidence whereas the a- and b-waves are defined with respect to the medium coordinate system. Therefore, when the plane of incidence changes the isotropic wave that couples to the biaxial wave also changes. We also observe that the imaginary part of the co-polarized transmission coefficient becomes non-zero beyond the critical angle. This behavior results in an evanescent wave in region 0 that decays rapidly as it propagates and is the cause of total internal reflection.

Next, the permittivity tensor is rotated around the x-axis by

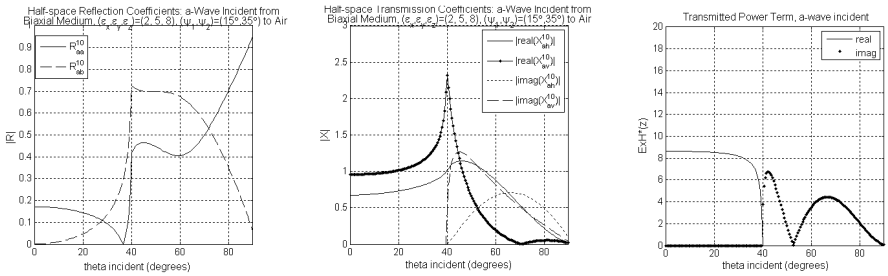

Figure 9. (a) Reflection coefficients for a-wave upward incident upon biaxial-air half-space. (b) Transmission coefficients for a-wave upward incident upon biaxial-air half-space. (c) Transmitted Poynting vector for a-wave incident from biaxial medium to air. Biaxial parameters: $(\varepsilon_x, \varepsilon_y, \varepsilon_z) = (2, 5, 8)$, $(\psi_1, \psi_2) = (15°, 35°)$.

15° (ψ_1) and around the z-axis by 35° (ψ_2). The resulting reflection coefficients are shown in Figure 9(a). We observe that depending on the angle of incidence, either biaxial polarization may be reflected more strongly. Also, we do not clearly see the total internal reflection as we did for the unrotated case. As the angle of incidence approaches 40°, the absolute value of R_{ab} rises dramatically to 0.7 with an absolute value of R_{aa} at approximately 0.45. Beyond 40°, the imaginary parts of both reflection coefficients become non-zero. We will see in our transmission and power analyses that 40° is the critical angle under this rotation. In the previous unrotated case the critical angle was 37.5° so the critical angle is affected by rotation.

In Figure 9(b), we plot the transmission coefficients for the rotated half-space problem. When the medium is rotated, energy is transmitted to both the horizontally polarized and vertically polarized waves in the isotropic region. This transmission is purely real until the angle of incidence reaches 40°. Beyond this critical angle, the transmission coefficients both become complex resulting in two evanescent waves and total internal reflection. The Poynting vector of the transmitted wave also shows that the critical angle occurs at 40° (Figure 9(c)). This figure also shows that the real and imaginary parts of the transmitted wave are both approximately zero at 52.5°. Finally, we analyzed the real transmitted and reflected power ratios and found that the total reflected power ratio goes to one at 40° verifying that 40° is the critical angle even if no one reflection coefficient is equal to 1. We also verified that power is conserved, showing that the sum of the two ratios is 1 for all angles of incidence.

3. TWO LAYER COEFFICIENTS

3.1. Derivation of Two Layer Coefficients

We can use the half-space coefficients derived in Section 2.1 to define two-layer coefficients. First, we use the half-space coefficients to define four half-space matrices. Note that in our derivation of half-space coefficients, we assumed all boundaries were at $z = 0$. However, for the two layer problem the second boundary (between region 1 and region 2) is located at $z = -h$ as shown in Figure 10. Therefore, a phase shift related to this z translation will have to be added to the region 1–region 2 coefficients. The resulting half-space matrices are given by

$$\bar{\bar{R}}_{01}^{(z=0)} = \begin{bmatrix} R_{hh}^{01} & R_{vh}^{01} \\ R_{hv}^{01} & R_{vv}^{01} \end{bmatrix}, \quad \bar{\bar{X}}_{01}^{(z=0)} = \begin{bmatrix} X_{ha}^{01} & X_{va}^{01} \\ X_{hb}^{01} & X_{vb}^{01} \end{bmatrix} \tag{8}$$

$$\bar{\bar{R}}_{10}^{(z=0)} = \begin{bmatrix} R_{aa}^{10} & R_{ba}^{10} \\ R_{ab}^{10} & R_{bb}^{10} \end{bmatrix}, \quad \bar{\bar{X}}_{10}^{(z=0)} = \begin{bmatrix} X_{ah}^{10} & X_{bh}^{10} \\ X_{av}^{10} & X_{bv}^{10} \end{bmatrix} \tag{9}$$

$$\begin{aligned} \bar{\bar{R}}_{12}^{(z=-h)} &= \begin{bmatrix} R_{aa}^{12} e^{i\left(k_z^{au} - k_z^{ad}\right)h} & R_{ba}^{12} e^{i\left(k_z^{au} - k_z^{bd}\right)h} \\ R_{ab}^{12} e^{i\left(k_z^{bu} - k_z^{ad}\right)h} & R_{bb}^{12} e^{i\left(k_z^{bu} - k_z^{bd}\right)h} \end{bmatrix}, \\ \bar{\bar{X}}_{12}^{(z=-h)} &= \begin{bmatrix} X_{ah}^{12} e^{-i\left(k_z^{ad} + k_{2z}\right)h} & X_{bh}^{12} e^{-i\left(k_z^{bd} + k_{2z}\right)h} \\ X_{av}^{12} e^{-i\left(k_z^{ad} + k_{2z}\right)h} & X_{bv}^{12} e^{-i\left(k_z^{bd} + k_{2z}\right)h} \end{bmatrix} \end{aligned} \tag{10}$$

We define the upward and downward propagating waves in each region as shown in Figure 10. We want to describe all of our two-layer coefficients as if a downward wave is incident from region 0 (the p-wave). We write each remaining wave in terms of the half-space

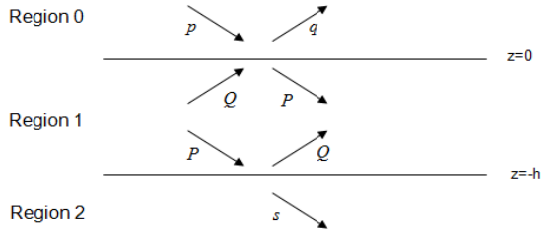

Figure 10. Incident, transmitted and reflected waves for two layer problem.

matrices in Equations (8) through (10). The resulting equations are

$$q = \left[\bar{\bar{R}}_{01}^{(0)} + \bar{\bar{X}}_{10}^{(0)}\bar{\bar{R}}_{12}^{(-h)}\left[\bar{\bar{I}} - \bar{\bar{R}}_{10}^{(0)}\bar{\bar{R}}_{12}^{(-h)}\right]^{-1}\bar{\bar{X}}_{01}^{(0)}\right]p \tag{11}$$

$$P = \left[\bar{\bar{I}} - \bar{\bar{R}}_{10}^{(0)}\bar{\bar{R}}_{12}^{(-h)}\right]^{-1}\bar{\bar{X}}_{01}^{(0)}p \tag{12}$$

$$Q = \bar{\bar{R}}_{12}^{(-h)}\left[\bar{\bar{I}} - \bar{\bar{R}}_{10}^{(0)}\bar{\bar{R}}_{12}^{(-h)}\right]^{-1}\bar{\bar{X}}_{01}^{(0)}p \tag{13}$$

$$s = \bar{\bar{X}}_{12}^{(-h)}\left[\bar{\bar{I}} - \bar{\bar{R}}_{10}^{(0)}\bar{\bar{R}}_{12}^{(-h)}\right]^{-1}\bar{\bar{X}}_{01}^{(0)}p \tag{14}$$

We consider overall reflection and transmission coefficients for this geometry with the wave incident from region 0. From Equation (11) we define the overall reflection coefficient matrix as

$$\bar{\bar{R}} = \left[\bar{\bar{R}}_{01}^{(0)} + \bar{\bar{X}}_{10}^{(0)}\bar{\bar{R}}_{12}^{(-h)}\left[\bar{\bar{I}} - \bar{\bar{R}}_{10}^{(0)}\bar{\bar{R}}_{12}^{(-h)}\right]^{-1}\bar{\bar{X}}_{01}^{(0)}\right] \tag{15}$$

From Equation (14) we define the overall transmission coefficient matrix as

$$\bar{\bar{X}} = \bar{\bar{X}}_{12}^{(-h)}\left[\bar{\bar{I}} - \bar{\bar{R}}_{10}^{(0)}\bar{\bar{R}}_{12}^{(-h)}\right]^{-1}\bar{\bar{X}}_{01}^{(0)} \tag{16}$$

3.2. Evaluation of Two Layer Coefficients

In this section, we analyze the two-layer coefficient in the same manner as detailed in Section 2 for the half-space coefficients. The biaxial layer (region 1) has a thickness of $0.4\lambda_0$ (where λ_0 is the free-space wavelength) and is situated between two isotropic regions both with permittivity and permeability of ε_o and μ_o respectively (air). In this analysis the biaxial medium has permittivity given by $\varepsilon_x = 3$, $\varepsilon_y = 4$, and $\varepsilon_z = 5$.

The first case we consider is the unrotated case in the x-z plane ($\varphi = 0°$). The two layer reflection and transmission coefficients are shown in Figure 11. The co-polarized reflection coefficients show that for all incident angles, the horizontal polarization is reflected more strongly, as is normally observed at an isotropic boundary. This is the same behavior discussed (but not shown) at the isotropic-biaxial half-space interface when the wave is incident from the y-z plane ($\varphi = 90°$). The cross-polarized reflection coefficients are approximately zero. Therefore, we observe similar behavior at the two-layer interface, with a different biaxial permittivity tensor, as we did in the half-space case. We also see that the vertically polarized wave undergoes zero reflection at the Brewster angle of 57.5°. Figure 11 also shows the calculated transmission coefficients. The co-polarized transmission coefficients have an inverse relationship to the reflection coefficients.

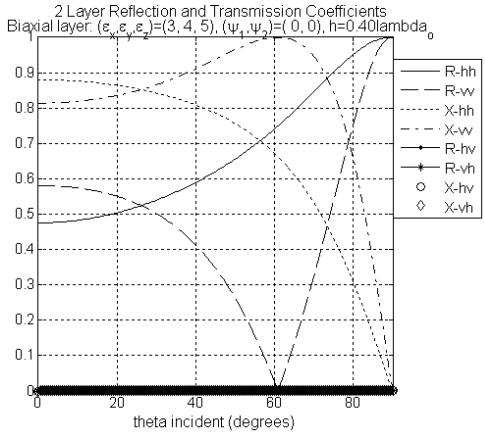

Figure 11. Two-layer coefficients for wave incident from the isotropic medium upon unrotated biaxial substrate.

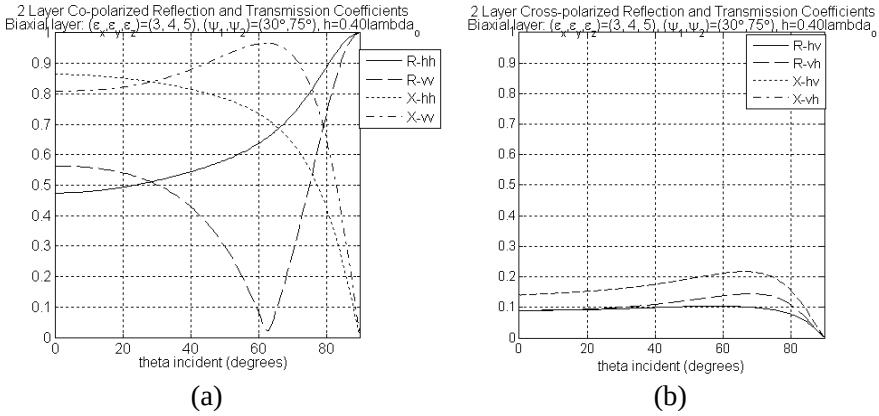

Figure 12. (a) Two-layer co-polarized reflection coefficients and (b) cross-polarized reflection coefficients for wave incident from the isotropic medium (region 0) upon rotated biaxial substrate $(\psi_1, \psi_2) = (30°, 75°)$.

We also see that the cross polarized transmission coefficients are also approximately zero. Once again, this is the same type of behavior observed in the half-space analysis where the a-wave acted as if it were co-polarized with the horizontal polarization and the b-wave co-polarized with the vertical polarization.

Once again we rotate the biaxial medium and observe the changes

to the reflection and transmission coefficients. In this case, we consider the same phenomena when region 1 is rotated by $\psi_1 = 30°$ and $\psi_2 = 75°$. Given this new biaxial medium, we first look at the co-polarized reflection coefficients shown in Figure 12(a). We observe that when the permittivity tensor is rotated, the vertically polarized wave is reflected more strongly than the horizontally polarized wave for small incident angles and that this behavior is reversed for larger incident angles. This behavior was discussed in the half-space problem where we observed this behavior with a rotation of 45° or more around the z-axis (ψ_2). Also, there is no true Brewster angle. The vertically polarized reflection coefficient has a minimum around 61° but does not go to zero. This is true in general of 2-layer problems. The co-polarized transmission coefficients have an inverse relationship to the co-polarized reflection coefficients. We also can see in Figure 12(b) that cross-polarized coefficients are non-zero. Note that the transmission coefficients overlap.

The two-layer reflection and transmission analysis is not complete unless we analyze the effect of thickness (or height) of the biaxial layer. We consider the same unrotated biaxial medium, this time with thicknesses of $0.02\lambda_o$ and $1.2\lambda_o$, with results shown in Figure 13. First, we consider the case of the very thin substrate (thickness is very small, $0.02\lambda_o$). The vertically polarized reflection coefficient (R_{vv}) is always less than the horizontally polarized coefficient (R_{hh}). The Brewster angle is the same as it was when the layer was $0.4\lambda_o$ thick (57.5°). The transmission coefficients are nearly 1 for low angles and zero for large incident angles and the cross-polarized coefficients are all approximately zero.

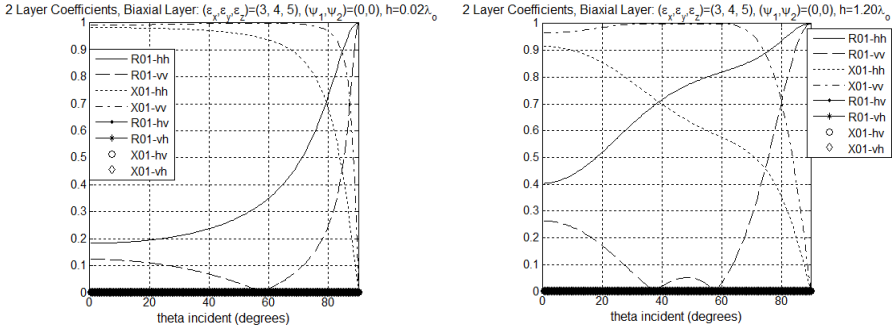

(a) (b)

Figure 13. Two-layer co-polarized reflection coefficients for wave incident from the isotropic medium (region 0) with biaxial substrate height of (a) $0.02\lambda_o$ and (b) $1.2\lambda_o$.

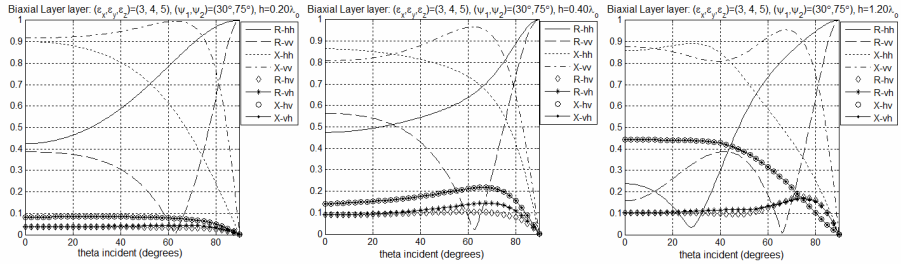

Figure 14. Two-layer co-polarized reflection coefficients for wave incident from the isotropic medium (region 0) with rotated biaxial substrates of varying heights.

When substrate is very thick ($1.2\lambda_o$) the vertically polarized reflection coefficient (R_{vv}) is still always less than the horizontally polarized coefficient (R_{hh}) and the cross-polarized coefficients are still nearly zero. Interestingly with this thick layer, we see what looks like two Brewster angles. One is at approximately the same angle observed at other thicknesses (57.5°), but there is another Brewster angle at 37.5°. This behavior is primarily due to the thickness of the layer as it may be observed when a thick middle layer is isotropic.

For completeness, we also want to consider the effect of varying the height of the biaxial layer when the medium is rotated. The results are shown in Figure 14. For all three heights, the cross-polarized reflection and transmission coefficients are significantly larger than in the unrotated case. As the height increases, these cross-polarized coefficients increase and may be greater than the co-polarized terms when the height is $1.2\lambda_o$. Not only do the cross-pol terms increase, but the minimum reflection coefficient for the vertically polarized wave is not zero. Finally, when the height of the anisotropic layer is $1.2\lambda_o$, both the horizontally and vertically polarized waves experience a type of Brewster angle effect.

4. CONCLUSIONS

In this paper we have investigated the reflection and transmission behaviors of electromagnetic waves at isotropic-biaxial interfaces. We considered half-space cases with waves impinging from either medium type and consider the two-layer case. We have presented a clear, general approach to deriving the reflection and transmission coefficients providing a more general approach than what is presented in [9, 10]. We showed that if a wave is incident from an isotropic region to a biaxial

region, the wave which is more strongly reflected can change. At small angles of incidence the vertically polarized wave may be more strongly reflected; as the angle of incidence increases, the horizontally polarized wave may be more strongly reflected. Although the vertically polarized wave may be more strongly reflected at small angles of incidence, it can still experience the Brewster angle effect and reach an angle of total transmission. This is completely different from anything observed at an isotropic-isotropic boundary. At these boundaries the horizontally polarized wave is always more strongly reflected than the vertically polarized wave. Even this unique behavior changes when the medium is rotated. Rotating the medium also results in double reflection and refraction, where a polarized incident wave will give rise to two reflected and refracted waves. This behavior is also not observed when both media are isotropic.

Unique behaviors are also observed in case of layered interfaces. When there are two layers (a biaxially anisotropic layer bounded by two isotropic layers), the vertically polarized wave can experience total transmission at more than one angle of incidence. This multiple Brewster angle effect was observed primarily due to the layer thickness. The effect of rotation on the layered case is similar to the half-space case in that double reflection and refraction is observed and the dominant reflected wave changes as a function of angle of incidence. In the case of the layered medium, we have defined a biaxial layer of any arbitrary thickness going beyond the thin film definitions in [14]. The wave formulation method of determining reflection and transmission characteristics at isotropic-biaxial interfaces provides straightforward theoretical analysis of biaxial media. This study demonstrates some of the unique behaviors of biaxially anisotropic media that may be applied when using either natural or manmade materials that demonstrate these characteristics.

Reflection and transmission coefficients not only provide physical insight into wave behavior, but they are also critical in studying electromagnetic devices. The eigenvector dyadic Green's function for biaxially anisotropic materials [11] has been used in [15] to study the behavior of microstrip antennas printed on biaxial substrates. This Green's function is based on the behavior of the waves at the interface between air and the substrate. The reflection and transmission coefficients are critical parameters in this Green's function and, therefore, critical to understanding physical devices implemented with biaxial substrates. Further, the knowledge of reflection and transmission coefficients can allow for better characterization of materials [16].

REFERENCES

1. Grzegorczyk, T. M., M. Nikku, X. Chen, B.-I. Wu, and J. A. Kong, "Refraction laws for anisotropic media and their application to left-handed metamaterials," *IEEE Transactions on Microwave Theory and Techniques*, Vol. 53, No. 4, 1443–1450, Apr. 2005.
2. Grzegorczyk, T. M., X. Chen, J. Pacheco, J. Chen, B.-I. Wu, and J. A. Kong, "Reflection coefficients and Goos-Hänchen shifts in anisotropic and bianisotropic left-handed metamaterials," *Progress In Electromagnetics Research*, Vol. 51, 83–113, 2005.
3. Kong, J. A., *Electromagnetic Wave Theory*, EMW Publishing, Cambridge, Massachusetts, 2000.
4. Tsalamengas, J. L., "Interaction of electromagnetic waves with general bianisotropic slabs," *IEEE Transactions on Microwave Theory and Techniques*, Vol. 40, No. 10, 1870–1878, Oct. 1992.
5. Semchenko, I. V. and S. A. Khakhomov, "Artificial uniaxial bianisotropic media at oblique incidence of electromagnetic waves," *Electromagnetics*, Vol. 22, No. 1, 71–84, Jan. 2002.
6. Lee, Y. H., "Microwave remote sensing of multi-layered anisotropic random media," Ph.D. Dissertation, Syracuse University, Syracuse, NY, Dec. 1993.
7. Stamnes, J. J. and G. S. Sithambaranathan, "Reflection and refraction of an arbitrary electromagnetic wave at a plane interface separating an isotropic and a biaxial medium," *J. Opt. Soc. Am. A*, Vol. 18, No. 12, 3119–3129, Dec. 2001.
8. Abdulhalim, I., "Exact 2×2 matrix method for the transmission and reflection at the interface between two arbitrarily oriented biaxial crystals," *Journal of Optics A: Pure and Applied Optics*, Vol. 1, No. 6, 655–661, Nov. 1999.
9. Landry, G. D. and T. A. Maldonado, "Complete method to determine transmission and reflection characteristics at a planar interface between arbitrarily oriented biaxial media," *J. Opt. Soc. Am. A*, Vol. 12, No. 9, 2048–2063, Sep. 1995.
10. Landry, G. D., "Transmission and reflection characteristics of biaxial interfaces in single and multilayer structures," Master's Thesis, The University of Texas at Arlington, Dec. 1993.
11. Mudaliar, S. and J. K. Lee, "Dyadic Green's functions for a two-layer biaxially anisotropic medium," *Journal of Electromagnetic Waves and Applications*, Vol. 10, No. 7, 909–923, 1996.
12. Pettis, G. F., "Hertzian dipoles and microstrip circuits on arbitrarily oriented biaxially anisotropic media," Ph.D. Dissertation, Syracuse University, Syracuse, NY, Dec. 2008.

13. Graham, J. W. and J. K. Lee, "Reflection and transmission at isotropic-biaxial interface," *30th URSI General Assembly and Scientific Symposium*, Istanbul, Turkey, Aug. 2011.
14. Adamson, P., "Reflection properties of a biaxially anisotropic dielectric film in a long-wavelength approximation," *Progress In Electromagnetics Research B*, Vol. 27, 37–59, 2011.
15. Graham, J. W. and J. K. Lee, "Microstrip dipoles printed on biaxial substrates," *2012 IEEE International Symposium on Antennas and Propagation*, Chicago, IL, Jul. 2012.
16. Valagiannopoulos, C. A., "On measuring the permittivity tensor of an anisotropic material from the transmission coefficients," *Progress In Electromagnetics Research B*, Vol. 9, 105–116, 2008.